Twist-averaged boundary conditions in continuum quantum Monte Carlo algorithms

C. Lin, F. H. Zong, and D. M. Ceperley
Department of Physics and NCSA, University of Illinois at Urbana-Champaign, Urbana, Illinois 61801
(Received 23 January 2001; revised manuscript received 3 March 2001; published 18 June 2001)

We develop and test Quantum Monte Carlo algorithms that use a''twist'' or a phase in the wave function for fermions in periodic boundary conditions. For metallic systems, averaging over the twist results in faster convergence to the thermodynamic limit than periodic boundary conditions for properties involving the kinetic energy and has the same computational complexity. We determine exponents for the rate of convergence to the thermodynamic limit for the components of the energy of coulomb systems. We show results with twist averaged variational Monte Carlo on free particles, the Stoner model and the electron gas using Hartree-Fock, Slater-Jastrow, and three-body and backflow wave function. We also discuss the use of twist averaging in the grand canonical ensemble, and numerical methods to accomplish the twist averaging.

DOI: 10.1103/PhysRevE.64.016702 PACS number(s): 02.70.−c, 82.20.Wt, 71.15.−m

Almost all quantum Monte Carlo (QMC) calculations in periodic boundary conditions have assumed that the phase of the wave function returns to the same value if a particle goes around the periodic boundaries and returns to its original position. However, with these boundary conditions, delocalized fermion systems converge slowly to the thermodynamic limit because of shell effects in the filling of single particle states. In this paper we explore an alternative boundary condition: one can allow particles to pick up a phase when they wrap around the periodic boundaries,

$$\Psi(\mathbf{r}_1+L\hat{\mathbf{x}},\mathbf{r}_2,\ldots)=e^{i\theta_x}\Psi(\mathbf{r}_1,\mathbf{r}_2,\ldots). \tag{1}$$

The boundary condition $\theta=0$ is called periodic boundary conditions (PBC), $\theta=\pi$ antiperiodic boundary conditions (ABC), and the general condition with $\theta\neq 0$, twisted boundary conditions (TBC) [1].

In periodic boundary conditions, the Hamiltonian is invariant with respect to translating any particle around the periodic boundaries. According to Bloch's theorem, this implies that any solution can be characterized by a given twist angle. The twist angle also has a physical origin: consider a toroidal geometry. One can either rotate the torus [2] and go into rotating coordinates, or add a magnetic flux [3] to the center of the torus. The physical properties will be unchanged. In both cases one can transform away the perturbation by applying TBC with the twist angle given by $\theta=mR^2\omega/h$ for rotation and $\theta=e\phi/(c\hbar)$ for magnetic flux. A torus is topologically equivalent to periodic boundary conditions, so that a nonzero twist will be allowed in periodic boundaries. The twist is a degree of freedom, or boundary condition, that can be varied to enable a finite system to approach the thermodynamic limit more quickly or to make a detailed studies of the properties of the quantum state.

If the periodic boundaries are used in all three directions, each dimension can have an independent twist [4]. Hence, in three dimension (3D), the twist is a three component vector, θ_i with $i=\{1,2,3\}$. The free energy and hence, all equilibrium properties are (triply) periodic [3] in the twist: $F(\theta_i+2\pi)=F(\theta_i)$ so that each component of the twist can be restricted to be in the range

$$-\pi<\theta_i\leqslant\pi. \tag{2}$$

For systems with a real potential (e.g., no magnetic field), one can further restrict the twist to be in the range $[0,\pi]$.

For a degenerate Fermi liquid, finite-size shell effects are much reduced if the twist angle is averaged over. We call this twist averaged boundary conditions (TABC) [5]. This is particularly important in computing properties that are sensitive to the single particle energies such as the kinetic energy and the magnetic susceptibility. By reducing shell effects, much more accurate estimations of the thermodynamic limit of these properties can be made. What makes this even more important is that the most accurate quantum methods have computational demands that increase rapidly with the number of fermions. Examples of such methods are exact diagonalization [6] (exponential increase in CPU time with N), variational Monte Carlo [7](VMC) with wave functions having backflow and three-body terms [8,9] (increases as N^4), and transient-estimate and released-node diffusion Monte Carlo methods [10] (exponential increase with N). Methods that can extrapolate more rapidly to the thermodynamic limit are crucial in obtaining high accuracy. Twist averaging is especially advantageous for stochastic methods (i.e., QMC) because the averaging does not necessarily slow down the evaluation of averages, except for the necessity of doing complex rather than real arithmetic.

The use of twisted boundary conditions is a common place for the solution of the band structure problem for a periodic solid. Band structure methods begin by assuming the wave function factors into single particle orbitals characterized by a lattice momentum. Then in order to calculate properties of an infinite periodic solid, properties must be averaged by integrating over the first Brillouin zone. Baldereschi [11] pointed out that in an insulator, in integrating over the Brilliouin zone, one can with high accuracy replace the integral with a ''special k point.'' This was generalized to a grid of k points [12]. Twisted boundary conditions has been discussed in connection with polarization of insulators [13]; we do not consider that here. The use of twisted boundary conditions is common in the analysis of lattice models [6,14]. Gammel [15] showed using perturbation arguments for certain lattice models why it will converge faster to the

thermodynamic limit and applied it to calculating optical properties. Gros [16] studied size effects in the Hubbard model with exact diagonalization and showed TABC gives exact results in the grand canonical ensemble for noninteracting systems.

Though twisted boundary conditions have a long history within quantum physics, their use in QMC has been limited [17]. In continuum QMC, Rajagopal and others [18,19] used special *k* points to reduce finite size errors for calculations of insulators within VMC. Their use in diffusion Monte Carlo (DMC) results were restricted to PBC and ABC in order to work with real wave functions. Králik *et al.* [20] used generalized boundary conditions to compute the momentum distribution with VMC for silicon (a semiconductor) and Filippi and Ceperley [21] did a similar calculation for metallic lithium. This was done in order to enlarge the number of momentum vectors in the region of the fermi surface. The use of TABC within QMC has not been further developed.

We focus in this paper on the use of TABC to reduce finite size effects (FSE) in the energy caused by the quantization of momentum with PBC. The FSE have been successfully corrected [17] for QMC by assuming that they are proportional to the finite size errors in a mean field method model such as Hartree-Fock or density function theory. In many cases, the largest finite size effects come from the Coulomb potential energy, in particular, due to the interaction of a charge with the correlation hole around its image in the periodic boundaries. Though these corrections are in most cases successful, we find a few examples, mainly in metals with strong electron correlation, where TABC allow a more accurate extrapolation to the thermodynamic limit.

We begin by discussing the method for noninteracting (NI) fermions. Fermi liquid theory asserts that the spectrum of states in an interacting fermion system is intimately related to those of the noninteracting fermion system, hence, a detailed analysis for the NI system carries over to strongly interacting fermi liquids. We then discuss interacting systems in the Hartree-Fock approximation: the electron gas and the Stoner model. In the Stoner model, we show how TABC can be used to determine a polarization phase transition at nonzero temperature. Results for TABC are given for the interacting electron gas using a pair product and backflow wave function in 3D. The electron gas system has been previously treated with an extrapolation method based on Fermi liquid theory. We show that TABC gives the same results in the thermodynamic limit and verify the applicability of the NI analysis, in particular, to examine how the energy depends on the twist of a given system size. We then present VMC results of the polarization energy of the electron gas using the new method and compare to the extrapolation method. In future publications we will study the low density properties of the electron gas using this technique. The Appendix discusses details arising in the implementation of TABC in QMC.

I. NONINTERACTING FERMIONS

In a noninteracting homogenous system with PBC, the single particle states are plane waves: $\exp(i\mathbf{kr})\,\eta(\sigma)$ where η is a spin function. For simplicity, we always assume the simulation cell is a cube (or square in 2D) of side L. To satisfy the twisted boundary conditions, the wave vectors obey

$$\mathbf{k_n} = (2\pi\mathbf{n} + \theta)/L, \tag{3}$$

where $\mathbf{n}$ is an integer vector. These states have energy $E_{\mathbf{n}} = (\hbar^2/2m)\mathbf{k}_{\mathbf{n}}^2$. The ground state in the canonical ensemble consists of the N lowest energy states; the many-body wave function is a determinant of those states. In this section we will ignore spin, since for a noninteracting system, spin modifies the results only by doubling the degeneracy of each level. Figure 1 shows the occupation of states for 13 spinless fermions in 2D for $\theta = 0$, i.e., with periodic boundary conditions, and also with a nonzero twist. The occupied states lie within a circle centered at the origin with radius $\approx k_F = 2(\pi\rho)^{1/2}$.

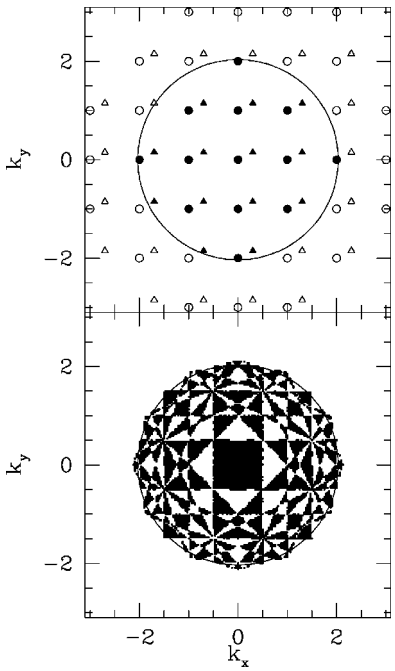

FIG. 1. Momentum distribution for 13 spinless fermions in a 2D square with side $L = 2\pi$. The top panel shows the occupied states (closed symbols) and empty states (open symbols) with zero twist (circles, PBC) and a twist equal to $2\pi(0.3,0.15)$ (triangles). The circle shows the infinite system fermi surface. The bottom panel shows the occupied states with TABC. The colored regions show the occupied region for the lowest level (middle square), the third level, up to the outermost 13th level.

Figure 2 shows the relative error in energy versus the number of fermions with PBC. The energy converges slowly to the exact result. One sees ''cusps'' in the curve at certain values of N. These occur at closed-shell values of N, e.g., the state depicted in Fig. 1 for PBC is a closed shell since states related by symmetry are either all filled or all empty. For large N the curve is ''quasirandom,'' with an envelope decaying algebraically as $N^{-\nu}$.

We find numerically that the exponent of the decay of the relative error of the energy is approximately, $\nu = 1.33$ in 2D

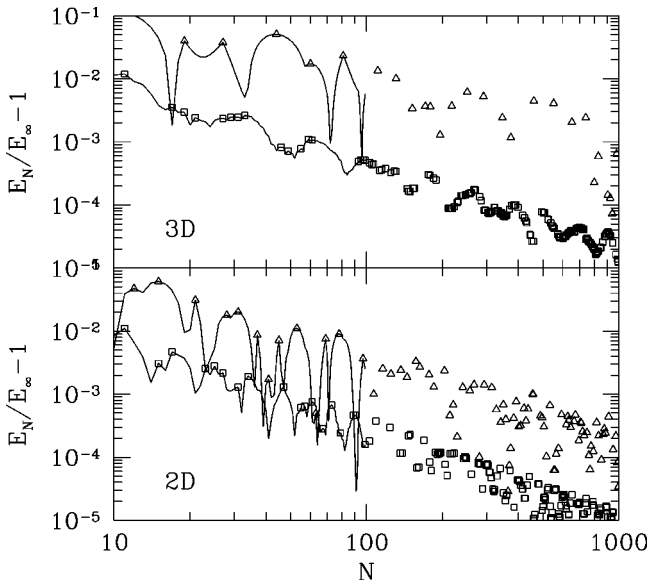

FIG. 2. Relative error of the energy versus number of particles with PBC (△) and TABC (□) in 2D and 3D. The points shown are only those where the relative error has a local maximum. Curves are shown only for $N<100$.

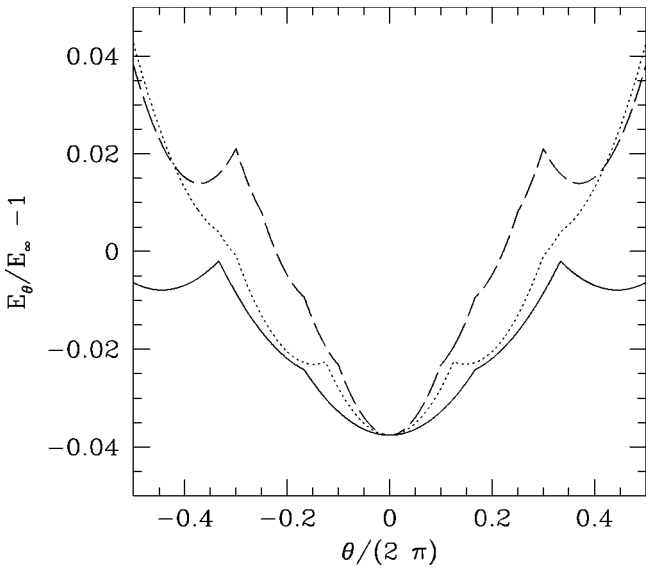

FIG. 3. Dependence of the energy of NI unpolarized fermions on the twist angle for $N=54$ in 3D. The solid line shows the energy along the (100) direction, dotted line along the (110) direction, and dashed line along the (111) direction. The curves are piecewise quadratic, with a cusp when the occupation of the states changes. We refer to the rms spread of energy values as the bandwidth.

and $\nu=1$ in 3D (see Table I). To characterize the approach to the thermodynamic limit, we introduce two different measures. Defining the relative scaled error δ_N as

$$E_N=E_\infty(1+N^{-\nu}\delta_N), \tag{4}$$

TABLE I. Coefficients of the asymptotic decay of the error in the relative NI energy. ν is the exponent of the decay. The exponents have been determined from the numerical data and are accurate to about 0.02. The amplitude was determined numerically by examining the values for $10\leqslant N\leqslant 10\,000$. The coefficients are defined as $a\equiv\max(|\delta_N|)$, $b=\langle\delta_N\rangle$, $c=\langle[\delta_N-b]^2\rangle^{1/2}$. n is the number of phase angles used for the summation in each dimension: $\theta_i=2\pi i/n$ for $i=1,\ldots,n$. $n=1$ corresponds to PBC; d is the dimensionality. O is the property: T, the kinetic energy; V, the Hartree-Fock potential energy of the electron gas; N, the number of particles in the twist average grand canonical ensemble (TA-GCE) method.

n	O	d	ν	a	b	c
1	T	2	1.33	4.5	0.37	1.77
8	T	2	1.5	0.47	0.27	0.093
1	N	2	0.67	2.18	0	0.65
16	N	2	0.75	0.71	0	0.52
1	V	2	1	0.50	-0.35	0.069
8	V	2	1	0.38	-0.367	0.0058
1	T	3	1	2.4	0.25	1.0
8	T	3	1.33	0.50	0.292	0.065
16	T	3	1.33	0.35	0.21	0.06
32	T	3	1.33	0.35	0.19	0.06
1	N	3	0.55	2.97	0	1.00
16	N	3	0.67	0.83	0	0.63
1	V	3	0.67	0.742	-0.549	0.072
16	V	3	0.67	0.587	-0.582	0.0043

we define $a=\max|\delta_N|$, $b=\langle\delta_N\rangle$, and $c=\langle(\delta_N-b)^2\rangle^{1/2}$. Table I shows estimates of these coefficients and exponents obtained numerically by examining values of $10\leqslant N\leqslant 10^4$.

Now consider twisting the boundary conditions, i.e., using a nonzero phase. This displaces the set of k vectors as shown in the top panel of Fig. 1. Aside from a set of special twists having zero measure, the energy levels will no longer degenerate. (When we sort the states to decide the filling, all states will have a different energy.) This is because inversion symmetry and rotational symmetry through 90° are broken. This breaking of symmetries and absence of degeneracies is a crucial difference between TBC and PBC.

At critical values of the twist, when a filled and empty state have the same energy, the occupation of the states changes. The condition for the degeneracy is that **k** lies on a plane bisecting and perpendicular to the line joining the origin with an integer vector; precisely the Laue condition for the Bragg planes [22] of the reciprocal lattice of the supercell. In Fig. 3 is shown the dependence of total energy on the twist angle for a fixed number of particles. One sees cusps as the filled states cross the Bragg planes. The dependence is similar to the band energy of a simple metal. Later, we will discuss this band structure for an interacting system. The bandwidth E_{BW} (the spread of energy values in Fig. 3) is defined as

$$E_{BW}^2=(2\pi)^{-d}\int d\theta(E(\theta)-E_\infty)^2 \tag{5}$$

and depends on the number of particles and scales as $E_{BW}\propto N^{-\nu}$ where the exponent ν is the same as describes the convergence of the kinetic energy in PBC.

There are several alternative procedures by which the twist angle can be varied: (i) one can average the twist over all possible values, (ii) the twist can become a dynamical variable, and (iii) special values of the twist could be used. Of these approaches, none are right or wrong in general; which method approaches the thermodynamic limit faster depends on the order of the phase in question, whether fermi liquid, ferromagnetic or antiferromagnetic. However, to compute a variety of properties for a metallic systems, we find the TABC best reduces size effects.

II. TWIST AVERAGING

The twist average of a property $\hat{A}$ is defined by

$$\langle \hat{A} \rangle = (2\pi)^{-d} \int_{-\pi}^{\pi} d\theta \langle \psi(R,\theta) | \hat{A} | \psi(R,\theta) \rangle, \tag{6}$$

where it is assumed that the wave function $\psi(R,\theta)$ is normalized for each θ. The momentum distribution, $n(\mathbf{k})$ is a key property to calculate for delocalized quantum systems. A discontinuity in $n(\mathbf{k})$ at the Fermi surface is responsible for the validity of Fermi Liquid Theory for metals. The kinetic energy is the second moment of the momentum distribution,

$$T_N = (\hbar^2/2m) \int d\mathbf{k} \mathbf{k}^2 n(\mathbf{k}). \tag{7}$$

Let us analyze the momentum distribution for NI fermions in the canonical ensemble. For any given twist θ, the N lowest energy states from those given by Eq. (3) are occupied. But any value of $\mathbf{k}$ can only be reached by a unique combination of $(\mathbf{n},\theta)$ if θ is restricted by Eq. (2). This proves that the averaged momentum distribution is a constant for states that can be reached by some combination of $(\mathbf{n},\theta)$ and zero otherwise. Hence within TABC, the set of filled states comprises a ''solid volume'' bounded by a Fermi surface. In contrast, for a single twist value, the momentum distribution is a point set. The total volume in k space inside the Fermi surface is precisely $(2\pi)^d \rho$, just as it is in the thermodynamic limit, so the constant is determined by the normalization condition,

$$\int d\mathbf{k} n(\mathbf{k}) = 1. \tag{8}$$

As mentioned above, the Fermi surface is a subset of the Bragg planes. For N particles the occupied states comprise the union of the first N Brillouin zones [22]. The $(N+1)$th electron will go in the $(N+1)$th zone, an area formed by planes surrounding the N^{th} zone. Figure 1 shows the momentum distribution of 13 spinless fermions in 2D using TABC.

In 1D, TABC gives the exact momentum distribution because the normalization condition determines everything. In higher dimensions the fermi surface is not perfectly circular (spherical) as shown in Fig. 1. However, one can see that $n(\mathbf{k})$ is much closer to a disk than the momentum distribution obtained with PBC. A perfect fermi surface (no finite size corrections) in any dimension, can be obtained by allowing variations in the particle number and working in the grand canonical ensemble as we discuss below.

Figure 2 shows the convergence of the error of the kinetic energy within TABC versus the number of particles. Numerical estimates of the relative error are given in Table I. One sees a dramatic improvement in the convergence with respect to PBC. The exponents governing the decay rate are larger and the errors are a factor of 30 smaller in 3D and 20 smaller in 2D for $N \approx 100$ (computed using exponents and a from Table I.) Note that the TABC kinetic energy must approach the exact energy from above. This is because the shape of a given volume with the smallest moment of inertia is a sphere, so that the distorted shape shown in Fig. 1 has a higher energy. Also shown in Table I is the dependence of the error on the number of twist values in the average. One needs from 16 to 32 values of θ along each axis to achieve the full reduction in size effects (better than a percent accuracy in the relative error of the size effects). In the Appendix are discussed the relative merits of performing the average on a grid versus sampling the twist values from a uniform distribution.

Let us now examine how the potential energy converges with PBC and TABC. This will give us some idea of how two particle correlations are affected by the boundary conditions since the potential energy is a particular integral over the pair correlation function. The calculation performed below is particularly simple for a power law potential, $v(r) = r^{-n}$. In particular, we examine the potential energy of an electron gas $(n=1)$ computed using the NI wave function (Hartree-Fock approximation). The NI trial function is valid for high density when the kinetic energy dominates the potential energy. The potential energy (using the Ewald image potential) is conveniently evaluated in Fourier space as a sum over the structure factor:

$$V = \frac{N\rho}{2} \sum_{\mathbf{k}} v_{\mathbf{k}} (S_{\mathbf{k}} - 1) + N v_M, \tag{9}$$

where v_M is the Madelung energy of a charge interacting with itself and $v_{\mathbf{k}}$ is the Fourier transform of the interparticle potential. For $1/r$ potential, $v_k = 2\pi(d-1)/k^{d-1}$. The values of $\mathbf{k}$ in the sum are given by $\mathbf{k} = \mathbf{2\pi n/L}$, where $\mathbf{n}$ is an integer vector. For the NI wave function, the structure factor at wave vector $\mathbf{q}$ is proportional to the probability that after we have displaced a filled state by $\mathbf{q}$ we are still in a filled state:

$$S_{\mathbf{q}} = 1 - \frac{1}{N} \left\langle \sum_{k<k'} \delta(\mathbf{k} - \mathbf{k}' - \mathbf{q}) \right\rangle, \tag{10}$$

where the sum is over occupied states and the average is over twisted boundary conditions.

Shown in Fig. 4 is the convergence of the potential energy versus the number of particles using PBC and TABC. For all values of N and twists the potential energy of the finite system approaches that of the infinite systems from below. Twist averaging serves to make the decay more regular but does not reduce its overall magnitude that is determined by a charge interacting with the correlation hole of its own image

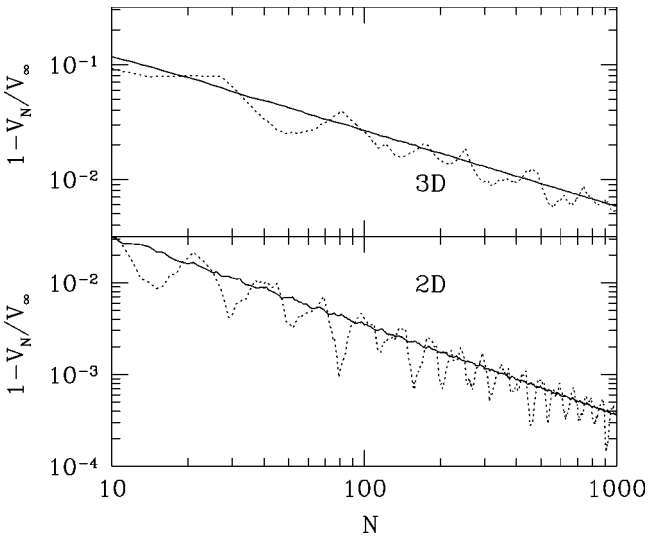

FIG. 4. Relative error in the evaluation of the potential energy for an electron gas using the Hartree-Fock wave function for N spinless electrons. The solid line shows TABC, the dashed line PBC.

in the nearby supercell. The smoother convergence obtained with TABC should allow for more accurate extrapolation to $N\rightarrow\infty$. Similar effects are expected for other two particle quantities.

III. GRAND CANONICAL ENSEMBLE

The use of TABC in the grand canonical ensemble (GCE) gives the exact single particle occupations for NI particles, as shown by Gros [16] within the Hubbard model. Suppose (α,N) is a label of the quantum states, both for the number of particles and for other quantum numbers such as the momentum and let $E_{\alpha,N}(\theta)$ be the energy of this state. Then the probability of a given state in the GCE is proportional to $\exp\{-\beta[E_{\alpha,N}(\theta)-N\mu]\}$ where μ is the chemical potential. In the ground state, $\beta\rightarrow\infty$, the occupied many-body state will be the one minimizing $E_{\alpha,N}(\theta)-N\mu$. Thus N can depend on θ.

We now show that for a NI system, twist averaged BC within the GCE give exact single particle properties; i.e., there are no finite size effects. Suppose the single particle energy levels are e_k. Then the probability of occupying the N states $e_1,\ldots,e_n$ is $\exp\{-\Sigma_{k=1}^{N}\beta[e_k(\theta)-\mu]\}$. In the occupation number $\hat{n}_k$ basis, this probability distribution factorizes as

$$\prod_{\mathbf{k}}\left[\hat{n}_k e^{-\beta[e_k(\theta)-\mu]}+(1-\hat{n}_k)\right], \tag{11}$$

so the probability of state k being occupied is precisely the fermi distribution law $n_k=\{\exp[\beta(e_k-\mu)]+1\}^{-1}$. As the twist angle is varied over its range, each momentum state of the infinite system occurs precisely once. Hence the averaged occupation number is precisely what it would be in the thermodynamic limit. The distortion of the fermi surfaces observed in the lower panel of Fig. 1 is a consequence of using the canonical ensemble.

The momentum distribution and hence the kinetic energy will be exactly equal to their infinite system values. Other properties may have finite size corrections; only the single particle properties are guaranteed to be exact. We call this procedure the twist average grand canonical ensemble (TA-GCE).

With this procedure one does not have a fixed number of particles since for a given twist and fermi wave vector, the number of occupied states will vary. The fluctuations in the number of particles is closely related to a famous problem in analytic number theory, ''Gauss's circle problem,'' to determine the number of lattice points inside a circle of area A as its radius tends to infinity [23]. As Gauss posed the problem, the center of the circle was fixed on a lattice site while in TA-GCE the circle is placed randomly (the shifted circle problem). It has been shown [24] that in 2D one obtains the following fluctuation in the particle number for TA-GCE:

$$\lim_{N\rightarrow\infty}\langle[N-(Lk_F)^2/4\pi]^2\rangle^{1/2}\propto N^{1/4}. \tag{12}$$

Our numerical estimates for the convergence are shown in Table I. Note that the Gauss circle problem differs from the convergence of the energy in the canonical ensemble since the energy is the average second moment of the lowest N points, not the number of points in a circle.

The preceding discussion refers to NI systems, however, fermi liquid theory asserts that the low lying excited states of an interacting system are in one-to-one correspondence with the NI states. Hence, as argued by Gross [16] and Gammel [15], TA-GCE is likely to reduce finite size effects substantially for interacting systems as well.

For an interacting many-body system, one difficulty in using the GCE is the need to optimize the wave function at each twist value; in particular to pick out which orbitals should be occupied. For an isotropic system having a spherical fermi surface, the order of filling the states is simple. For a metal with a nonspherical Fermi surface, the usual procedure is to determine the filling of single particle states according to a mean field theory such as the Kohn-Sham method in density functional theory. If one uses the same procedure within QMC, the Fermi surface will be substantially unchanged. Hence, it would be better to use that filling which minimizes $E_N-N\mu$.

There are other problems in using the GCE for charged systems in periodic boundary conditions. Usually the positive compensating charge, either a uniform background or a fixed array of charged nuclei, is at a fixed density. But if the number of electrons fluctuates, the periodic cell can have a net charge, which causes problems in calculating the long-range potential. Although very promising, we do not consider the TA-GCE method further in this paper. The following examples are for the canonical ensemble.

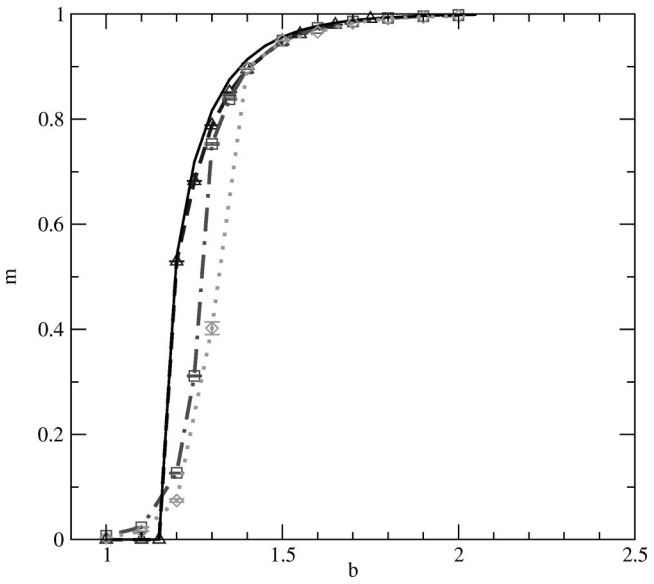

FIG. 5. Magnetization as a function of b for the 3D Stoner model. Circles are the exact results, diamonds for 54 electrons with PBC, squares for 54 electrons with TABC, and triangles for N=200 with TABC. The temperature was $T=0.224\ E_F$ and a 8^3 grid of twist values was used.

IV. THE STONER MODEL

To test the utility of TABC for determining a phase transition, we simulated the Stoner model, an analytically solvable model [25,26] for strongly correlated fermions, arising in the theory of itinerant magnetism [27]. The Stoner model differs from NI fermions by the addition of a contact repulsive potential: $\Sigma_{i<j} g\,\delta(r_{ij})$. The energy is evaluated within the mean field (Hartree-Fock) approximation using the NI wave function. For a spin (1/2) system, the potential energy is $E=E_{NI}+g n_\uparrow n_\downarrow$. In 3D the energy at zero temperature in the thermodynamic limit is

$$E/N=\lambda\frac{(3\pi^2\rho)^{5/3}}{10\pi^2}[(1+\zeta)^{5/3}+(1-\zeta)^{5/3}+b(1-\zeta^2)], \tag{13}$$

where $b=(5g\rho/6\lambda)(3\pi^2\rho)^{-2/3}$ and $\lambda=\hbar^2/2m$. For $b<1.111$ the system has an unpolarized ground state and for $b>1.3228$ the ground state is ferromagnetic. For intermediate couplings, the ground state has a partial spin polarization at zero temperature, similar to the behavior suggested [28,29] for the electron gas at low density.

We performed a MC simulation of the 3D NI system, within the occupation representation. The state variables of the system consist of occupation numbers (both spin and wave vector) and the twist angles. We make Monte Carlo moves consisting of flipping spins and moving the spatial occupation while keeping the particle number and twist angle fixed. If the new state is not already occupied, the move was accepted with probability equal to exp $\{-\beta[e_{new}(\theta)-e_{old}(\theta)]\}$. Figure 5 shows the convergence of magnetization distribution versus the number of fermions. We found that one could determine the phase transition within a few percent accuracy in the coupling constant b using only 54 fermions. Such accuracy within PBC would require thousands of fermions because of the strong shell effects.

V. ELECTRON GAS

We now present results for the 3D electron gas as a test of TABC on a correlated many-body continuum system. The electron gas is a very important model in condensed matter physics being the basis for the density functional theory method of electronic structure computations. [30,31] The phase diagram of the electron gas at low density is still not resolved [29]. The wave functions we use are the most accurate known for a continuum many-body system with optimized two-body, three-body, and backflow terms. VMC and DMC are QMC methods appropriate to zero temperature, and Path Integral Monte Carlo (PIMC) to $T>0$. In this paper, we will only discuss VMC and DMC. PIMC will be discussed in future publications.

In VMC, one assumes an analytic form for a trial function $\Psi_T(R)$ where R symbolizes the $3N$ coordinates. Then one samples $|\Psi_T(R)|^2$ using a random walk [7]. An upper bound estimate to the exact ground state energy is the average of the local energy $E_L(R)=\Psi_T(R)^{-1}\mathcal{H}\Psi_T(R)$ over the random walk. An accurate trial wave function is obtained from the NI wave function by multiplying with pair correlation terms. The pair product or Slater-Jastrow (SJ) wave function is

$$\Psi_2(R)=\mathrm{Det}(e^{i\mathbf{k}_i\mathbf{r}_j})e^{-\sum_{i<j}u(r_{ij})}. \tag{14}$$

One can determine the correlation factor $u(r)$ either with an analytic argument or by minimizing the energy and/or the variance of an assumed form. We use a parameter-free analytic form so that the systematic size and twist effects are not masked by noise in the trial function itself. For the electron gas an accurate analytic form for $u(r)$ based on minimizing the energy within the random-phase approximation [32] has as low an energy as those with optimized parameters. We used optimized Ewald sums [33] both for the potential and for the correlation factor so as to have the correct long wave length behavior.

Figure 6 shows the convergence of the VMC energy versus the number of particles within TABC and PBC. One can see the smooth convergence to the thermodynamic limit that was found within the NI system is also evident within VMC using the SJ wave function. We will discuss how to correct the much larger deviations of the PBC energy in the next section. The slow convergence of the TABC energy to the limit is due to finite size effects of the potential energy, computed with the Ewald summation method. This can be corrected using various procedures including simply extrapolation in inverse powers of N, or by using a modified interaction potential [19,38]. In addition to the Slater-Jastrow trial functions, we also have used optimized backflow-three-body functions (BF3B) [9] that give a more accurate description of the low-density electron gas. (They pick up about

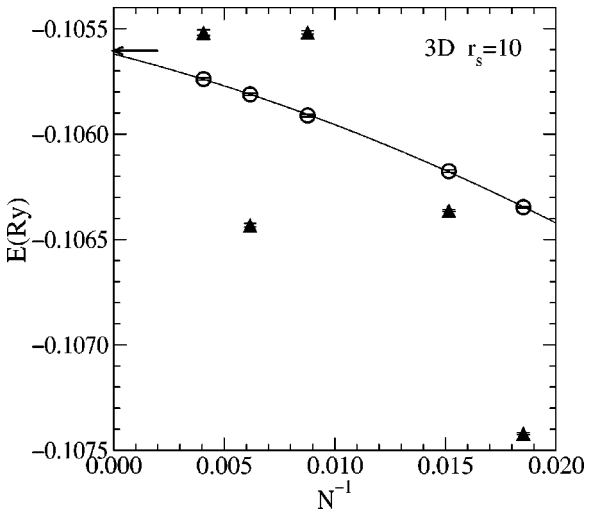

FIG. 6. Energy versus the number of electrons for the 3D electron gas using SJ wave function. The circles and connecting line are TABC with 10^3 twist values. The filled $\triangle$'s are using PBC. The arrow shows the extrapolation to an infinite system made using the PBC calculations using Eq. (16).

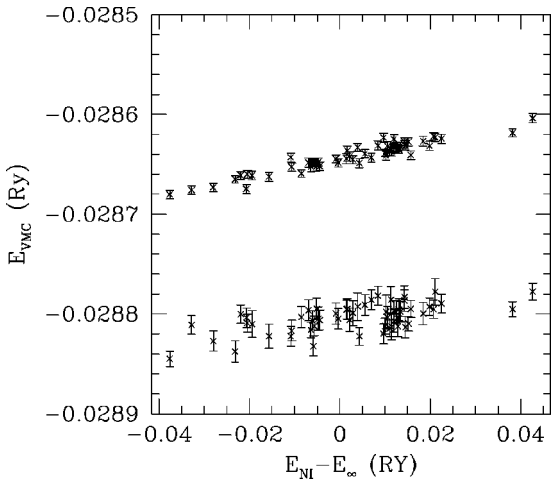

FIG. 7. Plot of the VMC energy versus the deviation of the NI energy from E_∞. Each phase angle is plotted separately. Simulations are for $N=54$ unpolarized 3D electron gas at $r_s=50$. Since the excitations are linearly related, Fermi liquid theory describes the phase angle dependence. Upper points are the Slater-Jastrow wave function, lower ones are done with the backflow-three-body trial function. Effective masses (the inverse slope) are respectively 1 and 0.61 for the two trial functions.

three-fourth of the remaining correlation energy [9] and break certain symmetries of the SJ wave functions.)

In the DMC method, one starts with a trial function and uses $\exp(-tH)$ to project out the ground state using a branching random walk. Fermi statistics pose a significant problem to the projection method, since exact methods such as transient estimate or release-node QMC suffer an exponential loss of efficiency for large numbers of particles. For this reason the approximate fixed-node method is normally used. Using the fixed-node method, one obtains the best upper bound to the energy consistent with an assumed sign of the wave function. Both the FN method and the exact transient estimate can be generalized to treat complex-valued trial functions [34]. These methods are called the fixed-phase and released-phase QMC. We have tried both of these approaches using TABC [35].

VI. FERMI LIQUID THEORY AND TABC

Fermi liquid theory (FLT) for metallic systems allows both a method to extrapolate to the thermodynamic limit and a way of understanding the twist dependence of the QMC results. According to Landau, the low-lying excitations of an interacting system are in close relation to those of the NI system:

$$E=E_0+\int d\mathbf{k}\,\delta n_{\mathbf{k}} e(\mathbf{k})+\int d\mathbf{k}d\mathbf{k}'\,\delta n_{\mathbf{k}}\delta n_{\mathbf{k}'} f(\mathbf{k},\mathbf{k}')+\cdots, \tag{15}$$

where $\delta n_{\mathbf{k}}$ is the deviation of the quasiparticle occupation from the ground state, and $e(\mathbf{k})$ and $f(\mathbf{k},\mathbf{k}')$ are one and two quasiparticle energy functionals. For simplicity we have not indicated dependence on spin. The energy functionals are usually further expanded about the fermi surface in spherical harmonics and applied to calculate properties in the thermodynamic limit. Here we discuss how to apply FLT when the ''excitation'' is caused by the boundary conditions. For example, we consider the momentum distribution shown in Fig. 1. The change in the energy caused by the noncircular shape should be given by Eq. (15).

We can analyze this dependence by comparing the energies of the noninteracting system within a given twist with the interacting system. This is done in Fig. 7 where we ignore the effect of the last term of Eq. (15). One sees a linear relation between the two energies, confirming that for these wave functions, Fermi liquid theory is an appropriate description. The inverse slope is proportional to the effective mass of the quasiparticles. Then since the NI infinite energy is known, this gives a way of determining the interacting system energy in the thermodynamic limit.

Previous calculations on the electron gas with PBC have used another application of FLT to correct for finite size effects: the extrapolation method [32,36,37]. In this method, one calculates ground state energies for a sequence of particle numbers, and determines the effective mass, potential correction, and infinite system energy by fitting these energies to the relation,

$$E_N=E_\infty+(m/m^*)\Delta T_N+\epsilon N^{-\nu}, \tag{16}$$

where ΔT_N is the deviation of the NI kinetic energy from the infinite system and ν is the exponent for the potential energy given in Table I. Figure 6 shows that the estimate of the infinite system energy obtained using TABC and the extrapolation method agree within errors. This is reassuring, but expected, since both are based on FLT. The TABC energies smoothly converge to the limit, even without FLT

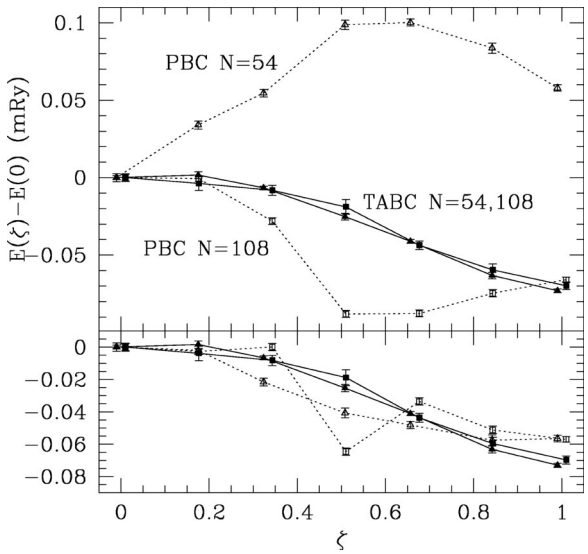

FIG. 8. Energy versus spin polarization for the 3D electron gas at $r_s=50$ computed with variational Monte Carlo with the Slater-Jastrow trial function using PBC (dotted line) and TABC (solid line). In the upper panel, no FLT correction has been made, so the PBC results for $N=54$ ($\triangle$) and $N=108$ ($\square$) differ by more than the polarization energy. In the lower panel, the PBC results have been corrected as in Eq. (16) with $m/m^*=1.6$, the value chosen to make the energy at $\zeta=1$ coincide. No correction has been applied to the TABC results in either panel. The twist values are sampled as described in the Appendix.

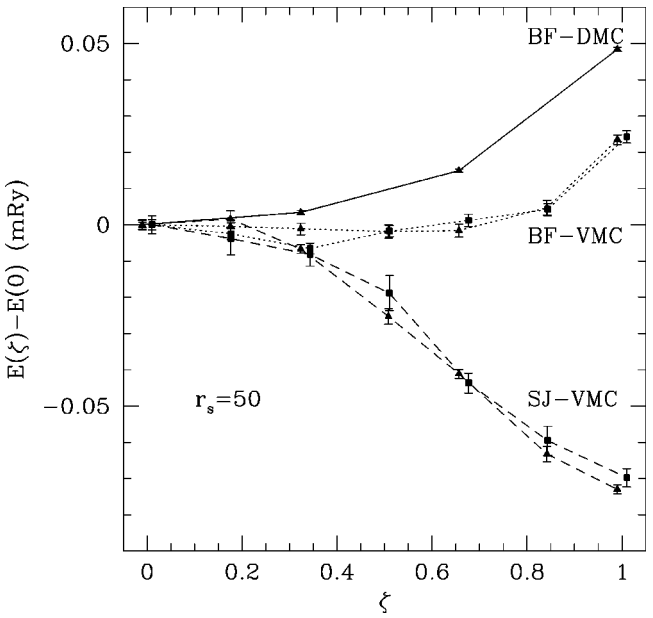

FIG. 9. Energy versus spin polarization for the 3D electron gas at $r_s=50$ within TABC. The solid line is using DMC with the BF3B trial function (grid of 10^3 twist values), the dotted line BF3B-VMC, and the dashed line SJ-VMC. The $\triangle$ is $N=54$, $\square$ $N=108$. The VMC calculations are done by sampling the twist values.

corrections. This smoothness allows one to determine the next order correction to the potential contribution, a term of order N^{-2}.

When it can be used, the extrapolation method gives precise results in the thermodynamic limit. However, there are significant advantages to the TABC method. The fitting method requires well converged runs for at least three different values of N. This can be difficult if the unit cell is large. For example, suppose one is doing a simulation of bcc hydrogen where one is limited to values of N equal to $2K^3=\{2,16,54,128,250\ldots\}$. The last three values are reasonable to simulate. But if the unit cell contained ten electrons, for example, the extrapolation using $\{540,1280,2500\}$ electrons would be very time consuming. Even more problematic is to use the extrapolation procedure on a liquid metal. One would have to perform an *ab initio* local-density approximation simulation of several different sizes of the liquid. There is also the problem that convergence and trial functions for large N may be inconsistent with those used for smaller N. For this reason, one typically determines m/m^* and ϵ within VMC and then applies the extrapolation using the DMC energies. This procedure will have additional systematic error.

There are other problems with extrapolation that we illustrate with the example of spin polarization. For example, suppose we have a partially spin polarized system with n_1 spin up particles and n_2 spin down particles. In Fig. 8 are shown comparison of computing the polarization energy at $r_s=50$ with both TABC and PBC. The upper panel shows the energy without FLT correction, the bottom panel assumes a best fit effective mass for PBC. The TABC energies can be used directly without correction and agree almost within error bars for systems of 54 and 108 particles, while the PBC has visible systematic effects even for 108 particles. In this example, the size effect of the potential energy is small because the pair correlation function is almost independent of polarization and thus cancels out of the polarization energy.

In Fig. 9 shows how the results of the polarization energy depends on the quality of wave function and the QMC technique, whether VMC or DMC. One sees that the good results of TABC are not due to the choice of trial function or QMC technique, but are quite general.

Within TABC, there is the possibility of obtaining results close to the thermodynamic limit, using only quantities computed for a single value of N, at least as concerns the finite size effects due to the kinetic energy. Other methods [19,38,17] are needed to make the potential correction. Use of TABC should allow these correction methods to be more accurate, because the structure factor and pair correlation function have more regular size effects as demonstrated in Fig. 4.

VII. OTHER PROCEDURES USING TWISTED BOUNDARY CONDITIONS

A. Dynamical twist method

As an alternative to TABC, one can let the twist angle be a dynamical variable (DTBC) and be determined self-consistently. By dynamical is meant that the probability of a given twist is proportional to its free energy:

$$P(\theta)\propto\exp[-\beta F(\theta)]=\sum_{\alpha}\exp[-\beta E_{\alpha}(\theta)], \qquad (17)$$

where $E_\alpha(\theta)$ is the energy of the state α with twist θ. This distribution of twist angles could be attained within QMC by enforcing detailed balance on moves of the twist angle during a random walk. The expectation of an operator A will be

$$\langle A\rangle_{DTBC}=\frac{1}{Z}\int d\theta e^{-\beta F(\theta)}\langle\Psi_\alpha(\theta)|A(\theta)|\Psi_\alpha(\theta)\rangle. \quad (18)$$

At zero temperature, a special set of twist angles, those that have the lowest energy, will be singled out, so that the ground state energy will be $E_{DTBC}=\min_\theta(E(\theta))$. Then for noninteracting fermions: $E_{DTBC}\leqslant E_\infty$, in contrast to the TABC that gives an upper bound for NI particles. In general, the dynamical energy, E_{DT} converges as slowly to the thermodynamic limit as does the PBC energy: the exponents and fluctuations are the same. The dynamical twist method is not an improvement over PBC for approaching the thermodynamic limit for a metallic system at temperatures much lower than the fermi temperatures.

Although the dynamic twist method is not satisfactory for a Fermi liquid at low temperatures, for certain lattice models such as an antiferromagnetic Heisenberg model, it can be a definite improvement over PBC and TABC. This is because one can only establish a defect-free Néel ordering if the unit cell is commensurate with the boundary conditions. For the Heisenberg model on a triangular lattice, the ground state has a given twist per lattice spacing. Using DTBC allows one to establish this twist value automatically, without imposing it in advance. This is equivalent to the classical variable cell method where the dimensions and aspect ratio of the supercell of a crystal become dynamical variables, so that one can determine the most stable crystal lattice structure [39] instead of examining each crystal structure explicitly.

B. Special points

For each value of N there exists a set of twist values for which $E(\theta)=E_\infty$. One can determine these special twist values for the NI system and then perform simulations at only one of those twist values for the interacting system, thereby getting rid of single particle size effects. This is similar to the special k point method of Baldereschi [11] for insulators where a single k point is determined by symmetry, thus allowing one to replace an integral over the Brillouin zone with evaluation at a single k point. This method was used within QMC by Rajagopal *et al.* [18] for solid germanium.

The special k-point method is advantagous if one evaluates an integral over a function that varies smoothly throughout the Brillouin zone and, as a result, is well approximated its lowest fourier components. This is appropriate for a filled band but not certain to work for a metal because the occupation number is discontinuous at the Fermi surface. Also, the ''special point'' cannot be specified in advance by symmetry because the location of the fermi surface can change between the interacting and noninteracting wave functions. In addition, it is not expected that the same twist values appropriate for the NI energy, will be appropriate for other quantities such as the potential energy, or spin susceptibility. It is better to have a method that can give a spectrum of properties correctly, rather than only a subset of properties. The use of special points will be better than using PBC but for correlated systems TABC will lead to higher accuracy. As we discuss in the Appendix, except for the problem of determining the phase dependence of the trial wave function, TABC does not impose an excessive computational burden, and is to be preferred over using only special twist values for strongly correlated metallic systems.

VIII. CONCLUSIONS

Note that there is a significant difference in the efficiency for stochastic (QMC) methods versus explicit methods such as density functional theory or exact diagonalization in regards to the TABC. In explicit methods, computations for each twist require an equal amount of computer time so that averaging over N_G twist values will take roughly N_G times as long as a single twist value. One can use inversion and rotational symmetry to reduce this, so that for a grid of 16^3 points with cubic symmtery, TABC will require only 165 twists. On the other hand, in QMC, all the twists reduce the statistical error of the average. The twists are simply three more degrees of freedom on top of the $3N$ coordinate variables to be averaged over. However, one must also take into account startup costs associated with each twist, such as reoptimizing the trial wave function or equilibrating the random walk. Neglecting these startup costs, there is no loss of statistical efficiency in performing TABC so that the gain in reducing the systematic error is free. This is examined in more detail in the Appendix.

There are many examples where twist averaging can effect considerable improvement over the use of PBC. We have been able to perform quite accurate calculations of the polarization energy of the 2D and 3D electron gas [35] and of liquid ^{3}He using backflow wave functions with on the order of 100 fermions. As pointed out by Ortiz *et al.* [29] calculations on such small systems in PBC have considerable systematic errors. Another related property that could be computed more accurately with TABC is the estimation of fermi liquid parameters by calculating particle-hole excitation [40]. TABC can reduce the shell effects that caused much difficulty in that calculation. A related example is in computation of the charge response of the electron gas [41] where a considerable effort was made to cancel out effects of the PBC. We are presently studying the electron gas confined to a slab [42] to determine the work function and surface energy of a metallic surface. The filled states consist of a set of disks, each of which will have a certain occupation number. By doing twist averaging we have shown reduced size effects with respect to PBC.

Experimental systems are at a nonzero temperature. For NI systems one occupies the states with probability given by the Fermi-Dirac distribution. Because the Fermi function at nonzero temperature is a continuous function, the convergence to the thermodynamic limit will be much faster, even with PBC. However in practice, one is interested in electronic systems close to the ground state; the relevant quantity is the thermal deBroglie wave length of the electron: $\hbar/(m_e k_b T)^{1/2}\approx 32$ Å at $T=300$ K. Because this length is

usually larger than the simulation cell in QMC, the localization of the density matrix does not help at reducing fermion finite size at these temperatures. Using a nonzero temperature just to achieve faster convergence to the thermodynamic limit is not practically useful. However, TABC is extendable to finite temperature PIMC simulations using the fixed-phase method [34] and will reduce size effects at low temperature.

The TABC method is likely to be valuable for all QMC calculations in systems with a fermi surface. The calculations on the electron gas demonstrate that even though it may be a little slower per step of the random walk, it is better to do TABC than a larger system with periodic boundary conditions because TABC converges much faster to the thermodynamic limit. The overall efficiency of any numerical method is ultimately judged by the computer time needed to reduce systematic and statistical error below a given value. TABC is effective in reducing the systematic errors and thus improve the overall efficiency.

ACKNOWLEDGMENTS

This research was supported by NSF DMR-98-02373 and the Department of Physics at the University of Illinois Urbana-Champaign. We acknowledge useful discussions with R. M. Martin and G. Bauer. Computational resources were provided by the NCSA. We thank H. Edelsbrunner for references concerning Gauss's circle problem.

APPENDIX

Here we discuss numerical details of implementing twist averaged boundary conditions. Many of the changes caused by twisted boundary conditions arise from the need to have complex wave functions. Although the wave function and energies in special cases are real (e.g., PBC and ABC), complex functions are needed for general twist angles. There is a factor of roughly 2.5 in additional CPU time to do the arithmetic to evaluate the determinant and its derivatives. The actual impact on the total speed is smaller than this because the calculations of two-particle quantities such as the potential energy and correlation factors are still done with real arithmetic; the actual penalty of working with nonzero twist depends on the number of particles and the type of trial wave function. However, as we have discussed earlier, even a factor of 2.5 in computer time is worthwhile if one is able to approach the thermodynamic limit quicker, since QMC methods scale as N^{ν} with $1 \leqslant \nu \leqslant 4$ or, in the case of exact fermion methods, as $\exp(\gamma N)$. If TABC saves going to larger N, the additional time doing complex arithmetic is well justified.

There are several alternatives for performing the twist averaging:

(1) Evaluate as $\Sigma_i w_i E_i$ using a grid defined by points θ_i with weights w_i (with $\Sigma_i w_i = 1$) in the region specified by Eq. (2).

(2) Sample the twist during the QMC random walk and take the average.

(3) A combination of the two approaches: working on a grid that is augmented with random displacements.

As we discuss below, all three methods are satisfactory; there is no fundamental difference in efficiency. The choice of whether to sample or use a grid is primarily based on convenience and programming considerations and only secondly on efficiency. We note that all methods are easy to parallelize.

1. Grid averaging

First, we must address the question of which grid and integration rule to use. Since all properties are periodic with respect to the twist, the grid should be a Bravais lattice with equally weighted points. One must keep in mind that the properties, though periodic and continuous, have discontinuous derivatives at the Bragg planes. Unless grid points can be located on these planes (which is difficult to achieve in practice), the integration error will go as $\epsilon_G \propto \Delta\theta^2 \propto N_G^{-2/D}$ where N_G is the number of grid points. Numerically, we find that 16^3 grids are needed for an accuracy of 10^{-3} (see Table I). This slowly convergent, systematic error is the main drawback of the grid integration method. For an insulator with a large enough gap to excitations, properties would be analytic for all θ since the occupation of single particle states will not change as a function of twist angle and the grid error would converge exponentially fast.

Once a grid is chosen, one can use symmetry (e.g., inversion and rotation through 90°) to reduce the number of grid points and give them a weight (w_i with $\Sigma_{i=1}^{N_G} w_i = 1$) proportional to their multiplicity. It is easy to show that the optimal amount of computer time at each grid point should be chosen proportional to $w_i/\zeta(\theta_i)^{1/2}$ where the MC efficiency at θ_i is defined as $\zeta(\theta_i) = 1/\{\mathrm{var}[E(\theta_i)] \times \mathrm{cpu\ time}\}$. We have found on the calculations of the electron gas described earlier, that this efficiency is independent of the twist angle except at the special PBC and ABC points where real functions can be used. Even though we have symmetry and can integrate over a reduced set of twist values, we must integrate longer at high multiplicity points since they contribute more to the average. Hence, the symmetry does not significantly reduce the needed amount of CPU time.

Since the calculations at different twist angles are uncorrelated, one can easily show that the efficiency of calculating the twist averaged energy is given by the relation,

$$\zeta^{-1/2} = \sum_{i=1}^{N_G} w_i \zeta^{-1/2}(\theta_i). \tag{A1}$$

Hence, the overall efficiency of the TABC energy is an average of the efficiencies of the individual twist calculations and is higher than that of the slowest converging twist angle. The additional averaging over twist angle costs nothing in efficiency.

This discussion did not take into consideration start-up costs at each twist angle, such as the need to reoptimize the trial wave function at a new twist value, and equilibration costs. By equilibration, we mean that whenever the twist angle is changed, enough random walk steps must be taken so that the configurations are sampled from the new twist value. During this equilibration, averages cannot be taken. These computational costs cause a decrease of efficiency by

the factor (useful time)/(total time) and are the main extra computational penalty of the TABC method within QMC. Since the start-up time will scale with the number of needed grid points, using the above estimate of the systematic error, ϵ_G, we find that the needed start-up time scales as $\epsilon_G^{-D/2}$ while the time to achieve equivalent statistical error scales as ϵ^{-2}. Hence, for very precise calculations ($\epsilon \to 0$) and $D<4$, start-up costs can be neglected. Many QMC calculations are dominated by the optimization of parameters in the trial wave function, so the start-up times of TABC will be prohibitive. However, it should be possible to reduce these start-up costs by using analytic properties of the trial function with respect to the twist.

2. Twist sampling

Now consider the second alternative, where the twist angle is sampled during the random walk. With this method, we do not have to decide on a grid in advance and there is no systematic error of a finite grid. Again, one must equilibrate the configurations after the change of twist angle and computer time used in that process does not reduce the variance of the average.

There is an additional increase in variance caused by sampling the twist angle. One can show that the efficiency decreases by a factor: $[1+E_{BW}^2/var(E_\theta)]^{-1}$ where E_{BW} is the ''bandwidth'' defined in Eq. (5). If one spends too long at a given twist angle, one is not adequately exploring the twist angle degree of freedom. This gives a definite rule for how often the twist angle should be updated: the time spent at a given twist angle should be much longer than the equilibration time but less than the time needed to get the error in the energy at that twist value equal to the ''bandwidth'' of the system. If it is not possible to achieve this relation, the grid scheme should be used.

With either method, one can achieve more accurate results and less systematic error by correcting the results using Fermi liquid theory. That is, using the twist values and corresponding energies one can estimate the effective mass and twist averaged energy using a least squares fit as discussed in Sec. VI. However, there will be additional statistical and systematic error resulting from the fit.

Finally, one can combine the positive features of two methods using antithetic sampling: use a relatively coarse grid, but then randomly displace the origin of the grid a number of times during the run, so as to eliminate the systematic error of the grid and estimate the true errors. Since the twist angle will change by a small amount, set-up time and equilibration time can be reduced. A related approach is to sample the twist angle using a quasirandom number sequence so as to reduce the dispersion of the twist values.

[1] We follow the usage of others in calling θ the *twist angle* rather than the phase angle to avoid confusion with all the other usages of the word phase that appear in quantum and statistical physics.

[2] A. J. Leggett, Phys. Fenn. **8**, 125 (1973).

[3] N. Byers and C. N. Yang, Phys. Rev. Lett. **7**, 46 (1961).

[4] Note also that all identical particles must have the same twist.

[5] This technique has also been called integration over boundary conditions (IBC) [16] and Phase Randomization [15].

[6] D. Poilblanc, Phys. Rev. B **44**, 9562 (1991).

[7] D. Ceperley, G. V. Chester, and M. H. Kalos, Phys. Rev. B **16**, 3081 (1977).

[8] Y. Kwon, D. M. Ceperley, and R. M. Martin, Phys. Rev. B **48**, 12 037 (1993).

[9] Y. Kwon, D. M. Ceperley, and R. M. Martin, Phys. Rev. B **58**, 6800 (1998).

[10] D. Ceperley and B. J. Alder, J. Chem. Phys. **81**, 5833 (1984).

[11] A. Baldereschi, Phys. Rev. B **7**, 5212 (1973).

[12] H. J. Monkhorst and J. D. Pack, Phys. Rev. B **13**, 5188 (1976).

[13] I. Souza, T. Wilkens, and R. M. Martin, Phys. Rev. B **62**, 1666 (2000).

[14] R. Jullien and R. M. Martin, Phys. Rev. B **26**, 6173 (1982).

[15] E. Y. Loh, Jr. and D. K. Campbell, Synth. Met. **27**, A499 (1988); J. Tinka Gammel, D. K. Campbell, and E. Y. Loh, Jr., *ibid.* **55-57**, 4437 (1993).

[16] C. Gros, Z. Phys. B: Condens. Matter **86**, 359 (1992); Phys. Rev. B **53**, 6865 (1996); R. Valenti, C. Gros, P. J. Hirschfeld, and W. Stephan, *ibid.* **44**, 13 203 (1991).

[17] W. M. C. Foulkes, L. Mitas, R. J. Needs, and G. Rajagopal, Rev. Mod. Phys. **73**, 33 (2001).

[18] G. Rajagopal, R. J. Needs, S. Kenny, W. M. C. Foulkes, and A. James, Phys. Rev. Lett. **73**, 1959 (1994); G. Rajagopal, R. J. Needs, A. James, S. D. Kenny, and W. M. C. Foulkes, Phys. Rev. B **51**, 10 591 (1995).

[19] L. M. Fraser, W. M. C. Foulkes, G. Rajagopal, R. J. Needs, S. Kenny, and A. J. Williamson, Phys. Rev. B **53**, 1814 (1996).

[20] B. Krlik, P. Delaney, and S. G. Louie, Phys. Rev. Lett. **80**, 4253 (1998).

[21] C. Filippi and D. M. Ceperley, Phys. Rev. B **59**, 7907 (1999).

[22] N. W. Ashcroft and N. D. Mermin, *Solid State Physics* (Saunders, Philadelphia, 1976), p. 162. The bisecting plane between the origin and any reciprocal lattice vector of the Bravais lattice are Bragg planes. The *n*th Brillouin zone is the set of points that can be reached from the origin by crossing exactly (*n*-1) Bragg planes.

[23] *Encyclopedic Dictionary of Mathematics*, edited by S. Iyanaga and Y. Kawada (MIT Press, Cambridge, 1980), p. 749.

[24] D. G. Kendall, Quarterly J. Math. **19**, 1 (1948).

[25] E. Stoner, Proc. R. Soc. London, Ser. A **165**, 372 (1939); **169**, 339 (1939).

[26] R. A. Suris, Sov. Phys. Solid State **3**, 1303 (1961).

[27] C. Herring, in *Magnetism*, edited by G. T. Rado and H. Suhl (Academic Press, San Diego, 1966), Vol. IV.

[28] B. J. Alder, D. M. Ceperley, and E. L. Pollock, Int. J. Quantum Chem. **16**, 49 (1982).

[29] G. Ortiz, M. Harris, and P. Ballone, Phys. Rev. Lett. **82**, 5317 (1999).

[30] D. M. Ceperley and B. J. Alder, Phys. Rev. Lett. **45**, 566 (1980).

[31] P. Hohenberg and W. Kohn, Phys. Rev. **136**, B864 (1996); R. M. Dreizler and E. K. U. Gross, *Density Functional Theory: An Approach to the Many-body Problem* (Springer, Berlin, 1990).
[32] D. Ceperley, Phys. Rev. B **18**, 3126 (1978).
[33] V. Natoli and D. M. Ceperley, J. Comput. Phys. **117**, 171 (1995).
[34] G. Ortiz, D. M. Ceperley, and R. M. Martin, Phys. Rev. Lett. **71**, 2777 (1993).
[35] C. Lin, Ph.D. thesis, University of Illinois Urbana-Champaign, 2000.
[36] D. M. Ceperley and B. J. Alder, Phys. Rev. B **36**, 2092 (1987).
[37] S. Fahy, X. W. Wang, and S. G. Louie, Phys. Rev. Lett. **61**, 1631 (1988).
[38] P. R. C. Kent, R. Q. Hood, A. J. Williamson, R. J. Needs, W. M. C. Foulkes, and G. Rajagopal, Phys. Rev. B **59**, 1917 (1999).
[39] M. Parrinello and A. Rahman, Phys. Rev. Lett. **45**, 1196 (1980).
[40] Y. Kwon, D. M. Ceperley, and R. M. Martin, Phys. Rev. B **50**, 1684 (1994).
[41] S. Moroni, D. M. Ceperley, and G. Senatore, Phys. Rev. Lett. **75**, 689 (1995); *Quantum Monte Carlo Methods in Physics and Chemistry*, edited by M. P. Nightingale and C. J. Umrigar (Kluwer, Dordrecht, 1999), p. 183.
[42] X. P. Li, R. J. Needs, R. M. Martin, and D. M. Ceperley, Phys. Rev. B **45**, 6124 (1992).